

The selection of an electric propulsion subsystem architecture for high-power space missions

*Original*

The selection of an electric propulsion subsystem architecture for high-power space missions / Paissoni, C. A.; Viola, N.; Andreussi, T.; Kitaeva, A.; Andrenucci, M.. - 2019:(2019). (Intervento presentato al convegno 70th International Astronautical Congress, IAC 2019 tenutosi a usa nel 2019).

*Availability:*

This version is available at: 11583/2837935 since: 2020-07-01T19:19:17Z

*Publisher:*

International Astronautical Federation, IAF

*Published*

DOI:

*Terms of use:*

This article is made available under terms and conditions as specified in the corresponding bibliographic description in the repository

*Publisher copyright*

(Article begins on next page)

IAC-19,D4,1,8,x53904

## The Selection of an Electric Propulsion Subsystem Architecture for High-Power Space Missions

Pissoni C.A.<sup>a\*</sup>, Viola N.<sup>b</sup>, Andreussi T.<sup>c</sup>, Kitaeva A.<sup>d</sup>, Andrenucci M.<sup>e</sup>

<sup>a</sup> Department of Mechanical and Aerospace Engineering, Politecnico di Torino, C.so Duca deli Abruzzi 24, Turin, Italy, 10129, [christopher.pissoni@polito.it](mailto:christopher.pissoni@polito.it)

<sup>b</sup> Department of Mechanical and Aerospace Engineering, Politecnico di Torino, C.so Duca deli Abruzzi 24, Turin, Italy, 10129, [nicole.viola@polito.it](mailto:nicole.viola@polito.it)

<sup>c</sup> Sitael S.p.A., Via Alessandro Gherardesca, 5, Ospedaletto (PI), Italy, 5612, [tommaso.andreussi@sitael.com](mailto:tommaso.andreussi@sitael.com)

<sup>c</sup> Sitael S.p.A., Via Alessandro Gherardesca, 5, Ospedaletto (PI), Italy, 5612, [alena.kitaeva@sitael.com](mailto:alena.kitaeva@sitael.com)

<sup>c</sup> Sitael S.p.A., Via Alessandro Gherardesca, 5, Ospedaletto (PI), Italy, 5612, [mariano.andrenucci@sitael.com](mailto:mariano.andrenucci@sitael.com)

\* Corresponding Author

### Abstract

The arise of high-power electric propulsion is paving the way towards new horizons of space exploration. Hall thrusters represent a promising propulsion concept, able to fulfil challenging mission requirements for both commercial and exploration applications. This technology offers several benefits in terms of flexibility of operation, extensive lifetime and high reliability. However, the design of a high-power electric propulsion subsystem (E-PROP) still presents challenges to address. Filling the corresponding technological gaps will open new market opportunities, owing mainly to the extension of mission capabilities and the reduction of the overall mission costs. Therefore, investigations of innovative technology alternatives will allow to identify the most promising E-PROP architectures for various high-power mission scenarios.

One of the most critical trade-off to perform is between a high-power monolithic thruster and a cluster of thrusters of lower power. Another criticality is the amount of propellant necessary to perform high delta-v missions. The high price of xenon prompted the investigation on alternative propellants, such as krypton. The propellant selection should consider the impact on different aspects of the platform design, including performance, system complexity and mission costs. Last, due to the high-power levels that the E-PROP shall manage, a different architecture can be implemented by adopting the direct-drive approach, i.e. a direct and non-isolated connection between the solar array and the thruster. However, even if the disruptive direct-drive technology allows a significant reduction in the EP system mass and cost, its implementation rises additional challenges to the design of the spacecraft power subsystem.

This paper analyses the impact of innovative architecture solutions on the design of a high-power E-PROP. In the framework of this research, we first carried out an extensive investigation of possible mission scenarios and we derived corresponding mission requirements and constrains. Then, we performed three technological trade-offs: monolithic 20 kW vs 5 kW cluster configuration, Xe vs Kr propellant and direct-drive vs standard PPU. All the analysis are based on the experimental data obtained during the 5 kW and 20 kW thrusters development and characterisation at SITAEL.

We characterized each design option through several figures of merit, evaluating them for each identified mission scenario. We exploited an Analytical Hierarchy Process for the trade-off analyses and a Monte Carlo method to perform the preliminary evaluation of the trade-off weights.

The analyses are based on the research activities that are currently ongoing at SITAEL and PoliTo in the framework of 20 kW E-PROP development programmes. The results of the work highlight the effects of each architecture alternative on both platform design and mission performance.

**Keywords:** electric propulsion, space tug, direct-drive, krypton, trade-off.

### 1. Introduction

In the recent years, High Power Electric Propulsion (HP-EP) has been identified as the most promising technology for enabling new and more challenging frontier in expansion of human presence in space. A vast majority of the research activities on HP-EP is now focused on the development and qualification of High-Power Hall Thruster (HP-HT), selected among the EP technology as the most suitable for future applications.

Several HP-HTs were developed and tested to investigate the operational features of these thrusters. In Europe, SITAEL is one of the main actors in high-power thruster-class field with the development of a 5kW-class and 20kW-class thruster, respectively the HT5k [1, 2] and the HT20k [3, 4].

These thrusters can benefit to mid and long-term space applications, in different operative environments. In particular, this technology is envisaged to be used on-board: (i) large telecommunication and navigation

satellites to perform electric orbit raising (EOR) manoeuvres to reach the final operative orbit, (ii) space transportation systems, to perform the transfer of cargo and supply materials between two orbits, (iii) for service platforms, to provide thrust mainly for both refuelling and deorbiting/disposal of platforms, (iv) for exploration and scientific platforms, as primary propulsion.

In order to implement more sustainable and affordable space missions, new transportation systems could be developed enhancing specific capabilities such as their reusability, to exploit them for more than one transfer, and their operational versatility, to use them for different purposes. These capabilities can converge in the adoption of a space tug, a reusable transportation system able to perform end to end transfers between two orbits. The payload transferred by the space tug could be identified either in a commercial satellite, to be transferred in its target operative orbit or in a cargo module, to resupply a space infrastructure such as a space station or an orbital refuelling station.

Taking into account these properties during the design phase, this typology of system will allow to reduce the mission cost, increasing mission sustainability and affordability with respect a possible future evolution of the chemical-based transportation system.

In previous works [5][6] all the applications listed have been analysed in different environments, identified in accordance with the Global Exploration Roadmap (GER2018) [7]. This process resulted in the development of 33 mission concepts each one characterized under both the system and the operational point of view. The starting and the target orbits, the refuelling orbit, the cargo mass transferred, and the traffic plan assumed, as well as the maximum transfer time were defined for each of the mission scenario identified. The HT20k was selected as reference thruster to be adopted on-board any of the platforms. The outcomes of these preliminary analyses were used to select a region on the operational envelope of the thruster where the majority of the mission concepts introduced turned out to fulfil the mission requirements and constrains defined during the mission analysis. However, few criticalities were identified in particular related to the system budgets. In order to perform multiple transfers, the space tug required a high propellant mass as well as the introduction of either dedicated systems or an infrastructure to provide refuelling capability in according to the selected refuelling strategy. Furthermore, the adoption of HP-HT required the generation of high power and the consequent dissipation of high heat loads derived from its processing. Lastly, for the fulfilment of the imposed mission requirements, a “high thrust” level was required.

This paper investigates possible solutions to mitigate these criticalities. Specifically, three different design choice were selected:

- 1) Monolithic vs cluster EPS architecture: the subsystem can be based on a single EPS string or multiple, string with a lower power. The cluster solutions can provide high-thrust level increasing the overall reliability of the EPS.
- 2) Kr vs Xe propellant operations: the adoption of different propellant could bring benefit in terms of costs even if different storing conditions shall be carefully investigated.
- 3) Direct Drive vs traditional PPU architecture: instead of feeding the thruster through a Power Processing Unit (PPU), a Direct Drive Unit (DDU) can be used. This has direct and indirect effects at system at subsystem level on all the operations.

The present analysis was performed in the framework of the EU’s H2020 Consortium for Hall Effect Orbital Propulsion System (CHEOPS) programme and an ESA/GSTP project with the MultidisciplinAry desiGN Electric Tug Tool (MAGNETO) tool [8], an upgraded version of the previous MISS tool, developed by Politecnico di Torino.

To investigate the adoption of the architecture alternatives previously listed, highlighting advantages and disadvantages in their adoption, a reference mission scenario was introduced. It consists in a transfer of a 2 tons commercial telecommunication satellite from its injection Low Earth Orbit (LEO) up to its final operative Geostationary Earth orbit (GEO). This typology of mission is still under particular attention by the operators due to the economic interest behind the possibility to provide telecom capabilities reducing the transfer costs. With the aim of comparing and identifying an optimal design solution, a trade-off process based on the Analytical Hierarchy Process (AHP) was implemented.

In this paper, after a detailed description of the alternative architecture under analysis and the definition of the thruster operative point (section III), the mission analysis performed on the selected reference transfer will be presented. After that, the design process based on MAGNETO tool will be detailed in section IV focusing on the upgrade of the design module necessary to assess the impacts of the alternative architecture on the platform design. The trade-off process definition along with the results obtained will be than presented in section V. Finally, section VI will report the main conclusion and the further developments of this analysis.

## 2. Mission profile

As previously defined, the different design solutions were studied analyzing their effects at mission, system and subsystem level through the definition of a reference scenario. The space tug approach allows to develop a mission concept where cyclical transfers between two orbits are envisaged. The reference mission was based on a LEO to GEO transfer of a commercial

telecommunication satellite. The mass of the satellite was fixed at 2 tons, considering the recent trend of reducing the GEO platform mass with the launch of platform such as Small GEO and ELECTRA [9][10]:

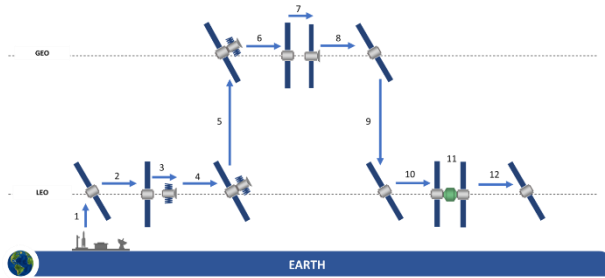


**Figure 1: Design reference Mission (DRM) of the LEO-GEO transfer reference mission.**

Figure 1 shows the mission profile selected as the reference scenario. After its launch into orbit, the space tug waits on a LEO parking orbit, waiting for the launch of the telecommunication satellite to be transferred. Then, in order to perform the rendezvous and docking (RVD) manoeuvre with the target telecommunication satellite, it has to assess its relative position with respect to the target telecom satellite. Once the RVD manoeuvre is concluded, the space tug has to wait the GO-command to perform the transfer up to the final GEO position defined by the operative requirements of the telecom satellite. When this position is reached, the tug releases the telecom satellite and performs a disengaging manoeuvre to move toward a safety position and starting the electric transfer phase back to the LEO parking orbit. Reaching the initial parking orbit, the space tug has to wait for the following launch of a telecom satellite to be transferred. During this waiting period, the refuelling operations take place through the availability of an On-orbit Refuelling System (ORS) which will be launched on the tug LEO parking orbit.

The refuelling operations are assumed to be performed at the end of every transfer in order to reduce the propellant mass unexploited during the transfer to GEO and, consequently, optimize the propellant consumptions.

Moreover, it is important to highlight that the space tug will be equipped with a chemical propulsion subsystem acting as actuators for the Attitude and Orbit Control Subsystem (AOCS). This subsystem is also used for the RVD manoeuvre in order to allow contingency manoeuvre for collision avoidance and to limit the degradation effects caused by plume impingement and contamination of the plasma beam, generated by the tug thrusters.

### 3. Architecture solutions

#### 3.1. Monolithic vs Cluster

To equip a spacecraft with a 15-25kW electric propulsion subsystem, it is possible to follow two different approaches:

- 1) Clustering 5 kW-class thruster units,
- 2) Using of a single monolithic 20 kW-class thruster.

Whereas the implementation of clustering may obviate the need to use thruster orientation mechanism (TOM), the monolithic option necessarily requires the application of TOM. This necessity complicates the thruster integration onto the platform and may have some impacts on the thermal management of the system.

Nevertheless, the clustering approach introduces several complexities in system integration, validation and operation, and the overall performance of the propulsion subsystem is typically lower than that of a monolithic thruster. As a matter of fact, to produce the same level of thrust, the cluster solution requires higher power levels with respect to the monolithic solution. This implies larger thrust-to-power ratios for the cluster option.

Moreover, direct sputtering erosion of inactive thrusters caused by firing of the active ones, is a great drawback of clustering, in particular for long operation times. Moreover, the clustering approach leads to a higher number of components leads to a greater complexity at system level, in particular for what concerns its (i) integration on the platform, due to the complex arrangement of the components, (ii) validation, due to the difficulties in testing a cluster and, (iii) operation, due to the complex thrust steering law to implement in order to avoid residual torque momentum on the spacecraft.

Moreover, the thruster arrangement has to be carefully evaluated in order to avoid thrust misalignment intrinsically derived from the geometrical disposition of the thrusters. Other aspects related to the integration complexity can be identified in the greater impact on the Thermal Control System (TCS) which has to manage heat flux generated by multiple hot spots.

On the other hand, the clustering approach introduces a greater flexibility in operation owing to the possibility to control independently each single EPS string. In some particular cases, this allows to obviate the use of thruster orientation mechanisms (TOM), controlling the thrust vector through an appropriate throttling of the thrusters. Furthermore, considering the throttling range of the single EPS string, a greater thrust range is obtainable.

### 3.2. PPU vs DDU

The conventional solution for EP systems is to use a power-processing unit (PPU) to modulate the energy produced onboard to meet the requirements necessary for Hall thruster operation in terms of current and voltage. Although PPUs have been used successfully in several space missions, the main drawback of these units is their relatively large size and mass. Apart from introducing an efficiency loss, the high power PPUs produce a significant amount of heat and therefore increase the workload of the spacecraft thermal management subsystem.

Another solution to deliver power to the Hall thruster is to directly transfer the energy generated by solar arrays to the thruster. This approach, which is called “Direct-Drive (DD)”, allows simplifying the PPU greatly, removing all power converters and implementing a simplified filter unit on the anode power line.

However, to benefit from the positive aspects of the direct-drive approach, it is necessary to develop satellite platforms with high bus voltages in the range of 300 to 500V, requiring high-voltage solar arrays and power bus. Moreover, the application of the high bus voltages implies that the satellite platforms would be more vulnerable to damages caused by charging. In addition, the PPU in conventional electric schemes serves as a galvanic isolator. Thus, non-isolated connection of the thruster to the solar arrays in the direct-drive scheme necessitates using appropriate filter units to damp out the possible large-amplitude oscillations in the thruster’s discharge current.

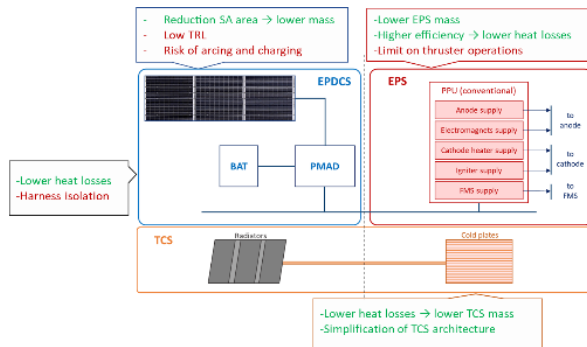


**Figure 2: schematic representation of advantages/disadvantages of the DDU implementation subdivided with respect to the subsystems mainly affected.**

In addition, the implementation of the DD approach necessitates the incorporation of new components in the spacecraft power system architecture, such as cathode return potential (CRP) power supply [11].

On a heritage perspective, SITAEL has performed an extensive experimental campaign aimed at characterizing

the controllability and stability of operation of its HT5k LL thruster using the direct-drive approach. One objective of the tests carried out was to quantify the values of CRP, which influences the amount of detrimental beam stray current towards spacecraft bus. Furthermore, three different control algorithms were developed and tested. The effectiveness of these algorithms in regulating the thruster behaviour was verified against representative variations in I-V characteristic curves of a solar array simulator.

Compared to the tests performed in SITAEL on the HT5k LL using conventional power supplies, the general conclusion from the experiments on the direct-drive HT5k LL was that no major differences exist in operating the thruster using the direct-drive approach.

### 3.3. Xenon vs Krypton

Krypton has physical properties close to those of Xe and a similar non-corrosive nature. These features, associated with krypton lower price, make it one of the most likely alternative propellants for the HET-based EPS, in particular for missions with high total impulse. The price of krypton is up to eighteen times lower than of xenon (Xe cost: 2200 €/kg, Kr cost: 120 €/kg [Latest quotation 01/2019]). However, due to its lower atomic mass with respect to xenon, the specific impulse for operation with krypton at the same voltage and power level is higher whereas the thrust is lower. SITAEL has already accomplished extensive experimental characterization of Hall thruster performance and behaviour with krypton. Krypton was used during the test campaigns with two Hall thrusters of different power levels, 5kW-class and 20kW-class [1, 4]. In particular, a dedicated series of tests have been performed under the ESA ARTES 5.1 program element to characterize the performance and erosion of the SITAEL’s HT5k thruster [12]. The operation with krypton showed a reduction in thrust and efficiency in parallel to an increase in specific impulse.

Another consequence of krypton lower atomic mass is reflected in terms of increased beam divergence. The beam divergence efficiency, when operated with Kr was reported to be 8% lower than with Xe [13]. Furthermore, due to the lower first ionization potential and higher ionization rate already at lower electron energies, Xe provides lower ionization cost and higher propellant utilization efficiency. At the same mass flow rate the propellant utilization for Xe was reported to be 5-10% better than for Kr [14]. As a result, the thrust-to-power ratio is typically lower for krypton. From the point of view of the plasma-wall interactions, compared to xenon, the krypton ions are accelerated to higher velocities in the same potential drop and, at the typical ion energies of HETs, the sputtering yield of the wall material increases for lighter particles. Hence, the erosion problem exacerbates with krypton. Moreover, in SITAEL, the

HC20 and HC60 cathodes, originally developed for Xe, were tested also with Kr. The cathodes proved to be completely compatible with Kr but operated with higher power consumption, due to the higher ionization energy of Kr [14].

Based on the results from the experimental campaigns and using the scaling model developed by Shagayda [15] the anodic specific impulse can be presented as a function of thrust for different power and discharge voltage levels. This approach was used to evaluate the operating parameters with Kr, used as initial conditions in the model.

What concerns system level aspects, xenon exhibits the high boiling point and high density at fixed pressure level. Therefore, it features a better storability than other potential propellants including krypton. To obtain Kr storage density above 1 kg/dm<sup>3</sup>, the krypton shall be stored at pressure above 250 bar, which implies higher challenges to the fluidic system and higher tankage fraction. However, the critical temperature of Krypton (T<sub>cr</sub>, Kr = -63° C, T<sub>cr</sub>, Xe = 17° C), provides a significant advantage from the point of view of thermal control.

### 3.4. Investigated architecture alternatives

The adoption of these alternatives was investigated considering a set of possible system architectures, representative for a trade-off analysis. The following table reports the selected cases:

**Table 1: alternative cases under analysis.**

	CASE #1	CASE #2	CASE #3	CASE #4
Monolithic	X	X	X	
Cluster				X
PPU	X	X		X
DDU			X	
Xenon	X		X	X
Krypton		X		

Starting from the baseline requirements previously defined two different sets of operative points for HT20k and HT5k thruster were identified and analysed for the architecture cases reported in Table 1. The two sets were chosen for better illustration of the effects of different parameters on the trade-off results and can be selected depending on the mission constraints and customer needs. Each of the four cases from Table 1 was analyzed then for both sets.

For the SET-1, the approach was to fix the values of the specific impulse and total EPS thrust. The corresponding thrust for each of the 5 kW thrusters in the cluster architecture was considered equal to 25% of the monolithic 20-kW one. The corresponding voltages and power discharge power level for both propellants were obtained from the SITAEL HT20k and HT5K

performance maps. As expected, the discharge voltage for the same thrust/specific impulse combination is lower for the system operating on Kr, while the discharge power is higher, due to the higher ionization losses with respect to the Xe case.

**Table 2: first set of thruster operative points.**

SET-1	HT20k Xe	HT20k Kr	HT20k Xe DDU	HT5k Xe
P [W]	21	22,5	21	6
T [N]	1	1	1	0,25
I <sub>sp</sub> [s]	2500	2500	2500	2250
V <sub>D</sub> [V]	450	375	450	600
m <sub>p</sub> [mg/s]	40,5	40,5	40,5	10,2

For the SET-2, the voltage and the total EPS power were fixed. For the cluster approach the power to each thruster was considered as 25% of the total power available for the EPS. The corresponding discharge power, thrust and specific impulse is presented in Table 3.

Due to the higher efficiency of the electrical subsystem, the Direct Drive approach allows higher power to be utilized for the plasma discharge and consequently higher thrust and specific impulse for the same operative voltage.

EPS on Kr with a traditional PPU provides higher specific impulse, lower thrust and lower mass flow rates with respect to the one on Xe.

**Table 3: second set of thruster operative point.**

SET-2	HT20k Xe	HT20k Kr	HT20k Xe DDU	HT5k Xe
P [W]	21	21	22,2	5,25
T [N]	1	0,77	1,06	0,26
I <sub>sp</sub> [s]	2500	3000	2550	2130
V <sub>D</sub> [V]	450	450	450	450
m <sub>p</sub> [mg/s]	40,5	26,4	42,4	12,4

## 4. Analysis process

After the identification of the mission scenario and its characterization in terms of functionalities, mission phases and operations, the system design definition proceeds with the sizing of the platform and its subsystems. For this step, an upgraded version of MISS tool has been developed and called MultidisciplinAry desiGN Electric Tug Tool (MAGNETO) [8].

### 4.1. MAGNETO tool

This software is a multi-input/output design tool which allows to define the mission scenario considering mission requirements and constraints derived from the



mission definition phase. The general architecture of MAGNETO tool is shown in Figure 3.

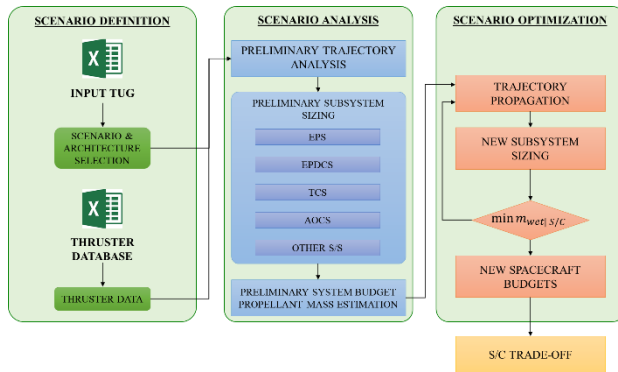


**Figure 3: simplified structure of MAGNETO tool.**

MAGNETO is based on three main modules: (i) scenario definition, (ii) scenario analysis and (iii) scenario optimization. In the first module, the mission scenario is introduced uploading two main databases. The first of them contains the subsystem design inputs through which the architecture of the different subsystems is defined, along with the identification and characterization of the mission phases. In particular, for what concerns the characterization of the mission phases, they are defined in terms of: (a) initial and final orbital values, (b) phase during which the telecom satellite is transferred and its mass, (c) maximum duration of the phase (for waiting phases only), (d) location of the refuelling operation and mass of propellant transferred.

During the scenario definition phase, the second database uploaded contains all the operative envelope of the considered thrusters. In fact, the tool has the possibility to analyse the operation of different typologies of HT, defining power level, thrust, specific impulse, propellant mass flow rate and voltage level for each desired operative point over the thruster operational map.

After the definition of both scenario and design input data, the initial design of the tug is performed in *Mission Analysis* module, where the main mission and system budgets are calculated. This preliminary sizing is based on “classical” subsystem models derived from [16], tailored with respect to the peculiarities introduced by the adoption of the electric propulsion technology. In particular, for what concerns the EPS sizing, it is possible either to select the data stored in a mass breakdown, if the thruster is known, or to base its sizing on a parametric model derived from a database of the thruster. The same approaches are exploited for the sizing of all the components of an EPS string: thruster, Power and Processing Unit (PPU), tank, pressure management assembly (PMA) and Flow Control Unit (FCU).

Furthermore, particular attention is given to the Electric Power Distribution and Control Subsystem

(EPDCS) and to the Thermal Control Subsystem (TCS) and the Attitude and Orbit Control Subsystem (AOCS). First, the EPDCS is designed considering the power budget of the tug during all the mission. It is calculated as a sum of the power of the EPS, the power of the other subsystems, considered with a percentage and additional safety margins proportional to the thruster power. The power generation function is in charge of solar arrays sized in terms of geometry and mass requirements. The batteries are instead considered for the storage of electrical power during eclipse period. Their sizing uses inputs coming from both the previous tool module and the preliminary analysis of the trajectories for the worst-case scenario. The AOCS and the TCS are sized considering the environmental conditions in which the tug has to operate. This allows to define the budgets of the system comprising passive components, actuators and sensors. This sizing phase is exploited in order to provide initial value for an optimization process performed in the last module of MAGNETO. In the *System Optimization* module, an iterative process allows to refine the mass of the spacecraft and optimized the propellant mass to be stored onboard the tug that affects the design of the tanks. Specifically, this optimization is performed exploiting a sequential algorithm, nested in an iterative cycle, able to identify the manoeuvres to perform during a specific phase and propagate the trajectory considering an imposed steering control law to identify the direction of thrust vector.

A set of weights for each orbital parameter is derived taking into account the values of the orbital parameters at each integration step, averaged by the difference between their initial and final values. This thrust steering law allows to obtain a suboptimal solution as demonstrated in [8]. After the propagation of the trajectories performed for each phase, the spacecraft is sized again in order to update the all the budgets. This process is then repeated up to convergence of the spacecraft wet mass within a determine tolerance range. The results obtained from the MAGNETO tool are compared through a trade-off analysis during the post-processing phase where a set of figures of merit (FoM) is evaluated in order to select the optimal system architecture.

#### 4.2. DDU design model

The DDU architecture design process is based on several modules introduced in the design process of the subsystems mainly affected by this peculiar system configuration, such as the EPS, the TCS, and the EPDCS.

For what concern the EPS, the main benefit of the DDU architecture with respect to the conventional PPU is the removal of the anode module(s). The mass savings provided by the DDU system can be, thus, evaluated as the difference in mass with respect to a classical PPU configuration. In addition to the anode module mass saving, the PPU mass is further reduced owing to the

smaller dimensions of both the chassis and the size of the TCS components necessary to dissipate the thermal load generated by the electronic components.

First, the anode module is designed as a single module of a conventional PPU in terms of a DC-DC converter, considered to be constituted by: (i) a chopper stage, which converts fixed DC input to a variable DC output voltage, (ii) an inverter transformer stage, to change the voltage output and provide isolation between input and output load, and (iii) a rectifier stage that provides rectified AC current to (iv) a downstream DC filter, whose output is a DC current to the Thruster Unit. A DC filter is placed upstream of all components to isolate the EPS from the EPDCS.

Figure 4 shows the conceptual arrangement of the components that form the PPU anode module.

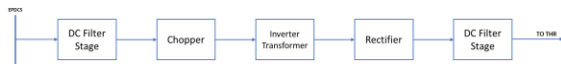


**Figure 4: Conceptual physical block diagram of a conventional PPU.**

To estimate the mass of a single anodic module, the model developed by NASA Glenn Research Center is used [17]. This model provides the mass trend evaluation of all electronic components, which constitute an EPS of a spacecraft, with respect to their sizing variables. Considering the models related to the components in Figure 4, the overall anodic module mass is obtained by summing over the corresponding mass of all components.

The design parameters introduced for the sizing of the electronic stages considered are hereafter listed:

- DC Filter stages: the input/output filter voltages and powers, the ripple factor, the filter efficiency (assumed equal to 99.8%), the switching frequency (assumed equal to 100 kHz) and the available/required module to define the internal redundancy logic (assumed equal to 3 required modules and 4 available modules assumed);
- Chopper stage: the input/output voltages and power levels, the switching frequency derived for the suggested values on [17], and the available/required modules assumed (3 required and 4 available modules assumed);
- Inverter/transformer stages: the input/output voltages and power levels, the switching frequency (in kHz) derived for the suggested values on [17], and the available/required modules assumed (3 required and 4 available modules assumed);
- Rectifier stage: the input power and voltage level, the stage efficiency (assumed equal to 98,7 % for stages operating over 110V) and the required available modules (3 required and 4 available modules assumed)

The Switching Frequency (SF) for both the Chopper and the Inverter/Transformer were derived using the suggested values in [17].

Another main advantage of the DDU system implementation is the reduction in mass of the TCS. As previously mentioned, the higher efficiency of the DDU system lowers the generated heat that needs to be dissipated by the TCS, which reduces the mass of the components necessary to collect transport and dissipate the heat loads. In particular, the design solution usually adopted for the conventional PPU architectures consists of heat pipe loops through which the heat flux generated by the PPU flows to either deployable or body-mounted radiators. In some specific architectures, the PPU is placed in contact with body-mounted radiators, therefore, avoiding the adoption of heat pipes loops. Due to the preliminary approach of the TCS design, the scheme with the heat pipe loops connected with body mounted radiators is considered. The TCS mass saving is assessed considering an average power specific mass of 28 kg/kW for the radiators and 14 kg/kW for the heat pipes loops [16].

Implementation of the DD approach introduces a high-voltage Electric Power Distribution and Control Subsystem (EPDCS), which provides high-voltage power to the EPS as well as to other subsystems on-board a spacecraft. High voltage EPDCS involves the adoption of the high-voltage solar arrays and batteries. All subsystems are supposed to be supplied by a high-voltage bus for their operation avoiding the increment in weight due to a step-down converter.

- *High-voltage solar arrays*

The selection of a high-voltage power bus necessitates the use of high-voltage solar arrays (SA). Despite the issues caused by the plasma environment surrounding the SA, as well as possible electric charging and arcing events, the implementation of a DD system allows a notable reduction in the SA area because of the higher efficiency of the DDU, and thus, the consequent reduction in the power demand required from the SA.

A review of the state-of-the-art in high-power SA showed that Ultraflex and Megaflex solar arrays developed by Orbital ATK are suitable for high-voltage operations [18][19]. These SAs have a specific architecture of the cells to increase the specific power, thus, increase the scalability to high power levels and feature innovative deployable system based on folding spar joints and panel extension hinges, allowing very high packing efficiency.

In order to estimate the indirect advantage of the DD system coming from the high-voltage SA, the methodology presented in [16] is followed. Table 4 summarizes the design parameters used in the analysis.



The SA area was calculated for the power levels required in both the PPU and DDU configuration.

As shown in Table 4, the lower power required by the platform because of DD system higher efficiency and lower losses through the power bus, translates in a reduction of the SA area. This has a direct effect also on the Attitude Orbit and Control Subsystem (AOCS) since the requirements on the torque force that it should counteract will be relaxed, therefore, resulting in the reduction of the subsystem mass. However, this effect is not included in this work.

**Table 4: SA design parameters.**

		NOTE
<b>Daylight time [s]</b>	5400	Worst condition LEO>GEO transfer
<b>Eclipse time [s]</b>	1800	Worst condition LEO>GEO transfer
<b>Daylight path efficiency (X<sub>D</sub>)</b>	0.85	[16]
<b>Eclipse path efficiency (X<sub>E</sub>)</b>	0.65	[16]
<b>Cell efficiency (BOL)</b>	33 %	Multijunction GaAS
<b>Inherent degradation</b>	0.805	[16]
<b>Specific power [W/kg]</b>	120	[18][19]

- *High-voltage battery*

The batteries represent one of the most critical issues for high-voltage EPDCS design. This is because of the fact that on the one hand, high-voltage bus could require several cells in series which increases the design complexity of this subsystem. On the other hand, adopting low-voltage batteries requires the use of a step-down converter. In this case, the subsystem mass savings and the reduction of generated heat load are lowered.

The Li-ion batteries were selected with an energy density of 130 Wh/kg [15]. This adoption of this typology of cells allows to reduce the number of cells necessary to operate at high-voltage level. The design of the batteries considers the worst-case scenario of eclipse during LEO to GEO transfer.

The power to be provided during the eclipse time is assumed to be 10% of the maximum power of the spacecraft. It is also pointed out that if a high-voltage EPDCS is selected, it allows the relaxation of this

requirement due to the lower power dissipation of the power bus.

Following the design methodology presented in [15], the design parameters taken into account are reported in Table 5.

**Table 5: Battery Design Parameters**

	PPU configuration DDU conf.	NOTE
<b>Eclipse time [s]</b>	1800	
<b>DOD</b>	0.75	[16]
<b>Transmission efficiency</b>	0.9	
<b>Energy density [Wh/kg]</b>	130	[16][20]

- *High-voltage power bus*

Adopting a high-voltage power bus for the EPDCS brings about other advantages at the spacecraft-level. In fact, a higher voltage bus can provide the same power level with a lower current, compared to a lower-voltage bus. Consequently, the ohmic heat dissipations ( $P_D = RI^2$ ) are reduced and thus, less heat shall be managed by the TCS. Assuming that 7% of total power is dissipated as heat [17] for a system based on PPU, the following ratio is defined to derive the power dissipated by a DDU-based system ( $P_{D,HV}$ ):

$$\frac{P_{D,HV}}{P_{D,LV}} = \frac{R I_{HV}^2}{R I_{LV}^2} = \frac{\left(\frac{V_{LV}}{V_{HV}} I_{LV}\right)^2}{I_{LV}^2} = \left(\frac{V_{LV}}{V_{HV}}\right)^2 \quad (1)$$

in which the indexes HV and LV denote High Voltage and Low Voltage, respectively.

#### 4.3. Store alternative propellant

When stored at the same pressure, Kr has much lower density than Xe. Therefore, it has a higher tankage fraction (the ratio between the tank and propellant masses  $m_t/m_p$ ) [13]. This means that much heavier and more voluminous tanks are necessary to store the same mass of propellant.

As a result of the trade-off between the tank volume and mass, Xe and Kr are typically stored at 186 bar and 300 bar respectively. To illustrate the effect of the difference in storage conditions on the tank mass (for the storage temperature of the 45°C), the results of the corresponding tank parameters, estimated for a reference mission case of 50 MNs, operative point defined in Case 1, are presented in Table 6.

The estimated titanium tank mass for Xe shall be of 209 kg versus 561 kg for Kr, and the tank volume shall be of 1082 l (Xe) versus 1798 l (Kr).

**Table 6: Xe vs Kr titanium tank parameters comparison.**

<b>Xe</b>			
	<b>Density</b>	<b>TF</b>	<b>M<sub>tank</sub></b>
	<b>[kg/m<sup>3</sup>]</b>	<b>(m<sub>t</sub>/m<sub>p</sub>)</b>	<b>[kg]</b>
P=186 bar	1884	<b>10.3%</b>	<b>209</b>
P=300 bar	2128	14.7%	299
<b>Kr</b>			
	<b>Density</b>	<b>TF</b>	<b>M<sub>tank</sub></b>
	<b>[kg/m<sup>3</sup>]</b>	<b>(m<sub>t</sub>/m<sub>p</sub>)</b>	<b>[kg]</b>
P=186 bar	751	25.7%	<b>525</b>
P=300 bar	1134	<b>27.5%</b>	561

The implementation of the composite overwrapped (COPV) tanks allows to reduce slightly the tankage fraction and, therefore, the mass of the tanks. Based on the available heritage, the corresponding typical COPV tankage fraction for Xe is about 8% and for Kr is about 17%. The results of the corresponding COPV tank mass is presented in Table 7.

**Table 7: Xe vs Kr COPV tank parameters comparison.**

<b>Xe</b>			
	<b>Density</b>	<b>TF</b>	<b>M<sub>tank</sub></b>
	<b>[kg/m<sup>3</sup>]</b>	<b>(m<sub>t</sub>/m<sub>p</sub>)</b>	<b>[kg]</b>
P=186 bar	1884	<b>8%</b>	<b>163.1</b>
P=300 bar	2128	9%	183.5
<b>Kr</b>			
	<b>Density</b>	<b>TF</b>	<b>M<sub>tank</sub></b>
	<b>[kg/m<sup>3</sup>]</b>	<b>(m<sub>t</sub>/m<sub>p</sub>)</b>	<b>[kg]</b>
P=186 bar	751	21%	346.6
P=300 bar	1134	<b>17%</b>	<b>428.1</b>

## 5. Architecture comparison results

In this section, the main results obtained by the previously introduced comparisons are described. First of all, the Analytical Hierarchy Process (AHP) with MonteCarlo weight derivation exploited for the comparison of the cases under analysis is presented. Then, the results obtained with MAGENTO tool and compared are presented for the all architecture cases introduced investigated for both sets of thruster operative points.

### 5.1. Trade-off definition

The trade-off methodology introduced follows the classical Analytical Hierarchy Process (AHP) where alternatives are compared through defined FoM for which weights and trade-off directions are assigned. Specifically, the FoM were selected considering the main parameters which intrinsically characterized the systems under analysis. The AHP proceeds with the definition of

trade-off weight for each FoM, usually selected between 1 and 9, with respect to the lower of higher importance of the FoM, respectively. A MonteCarlo process was implemented to assess the interdependency among the FoM weights. This implies to define a range of values for each weight varying between a minimum weight value up to a maximum desire value. Lastly, the direction of the FoM depends on the desire to minimize or maximize the FoM value. As a result, in

<b>Figure of Merit</b>	<b>W<sub>min</sub></b>	<b>W<sub>max</sub></b>	<b>DIR</b>
S/C Dry mass	8	9	LOW
Propellant mass	8	9	LOW
Total mower	7	9	LOW
Delta-V	6	8	LOW
Total transfer time	8	9	LOW
Outward transfer time	5	6	LOW
EPS cost	7	8	LOW
Propellant cost	7	8	LOW
EPS reliability	6	9	HIGH
TRL	7	9	HIGH
Complexity	6	8	LOW

, all the FoMs, weights, directions and assumptions made are reported. Moreover, the FoM related to each comparison under analysis are identified since not all of them were evaluated for each comparison.

**Table 8: Weight ranges (W<sub>min</sub>,W<sub>max</sub>) and direction for each FoM.**

<b>Figure of Merit</b>	<b>W<sub>min</sub></b>	<b>W<sub>max</sub></b>	<b>DIR</b>
S/C Dry mass	8	9	LOW
Propellant mass	8	9	LOW
Total mower	7	9	LOW
Delta-V	6	8	LOW
Total transfer time	8	9	LOW
Outward transfer time	5	6	LOW
EPS cost	7	8	LOW
Propellant cost	7	8	LOW
EPS reliability	6	9	HIGH
TRL	7	9	HIGH
Complexity	6	8	LOW

The main assumptions and the methodology followed for the definition of a numerical value for each FoM in the different architecture considered are briefly listed hereafter:

- **S/C DRY MASS:** the evaluation performed considering the mass breakdown of the single components of the EPS. the ESA margin philosophy [21] was considered for taking into account uncertainties on the integration onboard the platform.
- **PROPELLANT MASS:** this FoM is evaluated through the trajectory propagation routine in

MAGNETO. It strongly affects the design of the propellant feeding line, in particular for what concern the tank. As detailed in the previous paragraphs, an extensive investigation on the COTS tank was carried out in order to derive the tankage fraction for both xenon and krypton.

- **TOTAL POWER:** the power budget results from the design of the system. In the case of the space tug, its value is directly derived from the power consumed by the EPS which represents the main load of the spacecraft. In MAGNETO, the total power is calculated considering the power consumed by the EPS with an additional external load of 10% for the other subsystem of the tug. Moreover, an additional safety margin is considered.
- **TRANSFER TIME:** this FoM is of crucial importance for the customers due to their need to have their satellite in operation as soon as possible. To taking into account this constrains as well as the availability of the tug for the following trips, two transfer time values were considered in the trade-off. First, the outbound time necessary to transfer the satellite for its capture in the launch deploy orbit up to its operative position. This period could be interpreted by the customers as the “time-to-market” of the satellite after the launch phase. Second, the total transfer time which defines the period between one transfer and the following, setting the availability of the space tug during its operative lifetime. Both FoMs were evaluated through the trajectory propagation routine of MAGNETO.
- **DELTA-V:** as an output of the propagation routine of MAGNETO, the delta-V can be easily derived for each transfer. As defined in [8], the thrust steering control law introduced allows to obtain a sub-optimal solution.
- **EPS STRING COST:** the cost of an EPS string is calculated through the model introduced by Hofer in [22]. The growth percentage considered in the model foreseen an increasing of two time of the total cost of the string every 10 kW.
- **PROPELLANT COST:** the propellant cost is derived during the post-processing of the MAGNETO results. To establish the final value, the last quotations, previously defined, are used. Any additional costs are considered for the propellant delivered from the ORS to the tug.
- **EPS RELIABILITY:** the reliability of the EPS architecture is defined considering a fixed value for the entire string. A value equal to 0.95 is introduced in a “K out of n” model for the calculation of the different subsystem reliabilities (monolithic vs cluster only). Any redundant thruster is included.
- **TRL:** this value is defined considering actual development status of the technologies under analysis.

- **COMPLEXITY:** this FoM takes into account the (i) integration, (ii) validation and (iii) operational complexities.

Equation (2) was implemented to derive the weight of each FoM considering the MonteCarlo approach.

$$W_h = \frac{\sum_{k=1}^N \left( \frac{rand(W_{min |i}, W_{max |i})_k}{\sum_{q=1}^M rand(W_{min |i}, W_{max |i})_q} \right)}{N} \quad (2)$$

where N is the number of MonteCarlo random cases, M is the FoM index and W is the weight calculated for each h-th FoM.

The final scoring for the two architecture is obtained with the following expression:

$$S_i = \sum_{h=1}^M \delta_h \cdot W_h \cdot V_{hi} \quad (3)$$

where  $S_i$  represents the final score of the i-th case under comparison,  $\delta_h$  is the direction of trade-off defined for each h-th FoM,  $V_{hi}$  is the i-th FoM normalized value.

### 5.2. SET-1 of operative points: architecture comparison results

In this section, the comparison of the most relevant FoM is shown highlighting the relative percentages with respect to the reference architecture identified as monolithic-PPU-Xe.

Figure 5: Results of the Dry Mass and Propellant Mass budgets comparison, SET-1. Figure 5 reports the mass budgets of the platform. Due to the higher number of components, the space tug with a cluster EPS configuration has a higher dry mass than the monolithic configuration. The architecture based on krypton propellant results in a higher dry mass, with respect to the xenon-based architecture, due to a higher krypton tankage fraction.

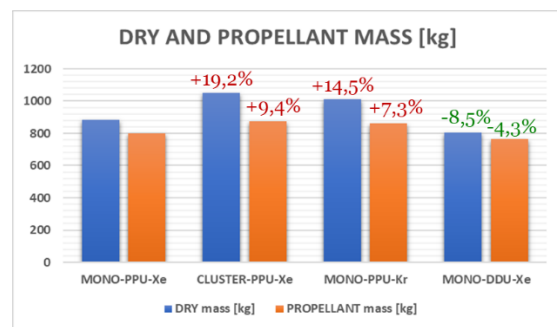
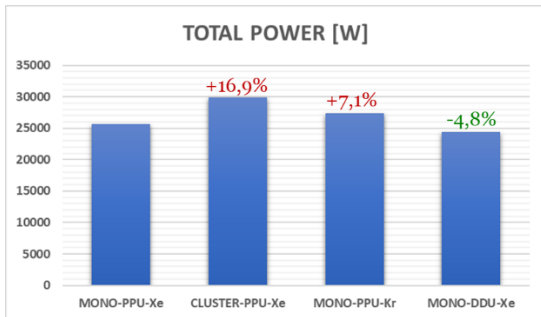


Figure 5: Results of the Dry Mass and Propellant Mass budgets comparison, SET-1.

On the contrary, the lower mass obtained with the DDU configuration comes as a direct consequence of the simplification of the power and thermal subsystems of the tug and their relative reduction of mass. For all the cases, the propellant mass is reported in Figure 5 with orange bars.

The architecture comparison for the propellant mass follows the trend of the one obtained for the dry mass. The propellant mass results to be slightly lower than the dry mass for each architecture. This result is obtained due to the peculiar operation of the tug which has to perform a round transfer to return back in its initial parking orbit. Considering the outbound trip only, the relative percentage of propellant mass results lower than 30% for all the configurations. Same trends are followed by the power budgets (Figure 6). The power demand increases when cluster or krypton-based architectures are chosen, while a saving of around 5% of power can be achieved with the DDU architecture. This advantage is obtained owing to the greater efficiencies of the power subsystems when operating at higher voltages due to the lower losses from the Joule effect on the power lines.



**Figure 6: Total Power Budget comparison, SET-1.**

Through the trajectory propagation routine of MAGNETO, the transfer time was evaluated considering the reference operation of the space tug defined in the previous sections.

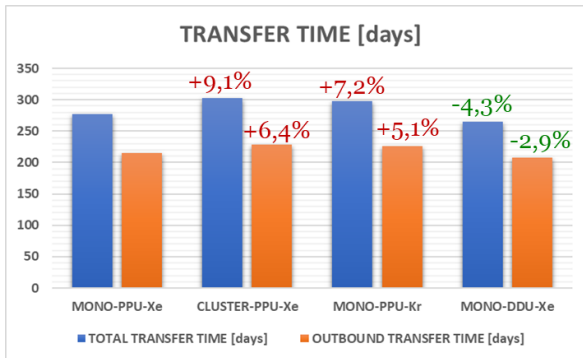


**Figure 7: Total and Outbound transfer time comparison, SET-1.**

The results are subdivided in total and outbound time transfer (blue and orange bars respectively in Figure 7). In particular, the outbound transfer time is reported because it can be interpreted as the “time-to-market” of the satellite after its deployment from the launch vehicle. Due to the higher wet masses, greater total transfer times were obtained for cluster and krypton configurations (on 9% and 7% respectively with respect to the reference configuration).

The propellant cost is a FoM which has one of the most important impacts on the final result of the comparison. Figure 8 shows that a reduction of over 94 % of the propellant cost can be obtained using krypton propellant. These results include only the cost of the first-round trip of the space tug.

Finally, exploiting the trade-off methodology introduced in the previous section, each architecture was compared with the reference architecture: monolithic, PPU and xenon operation.

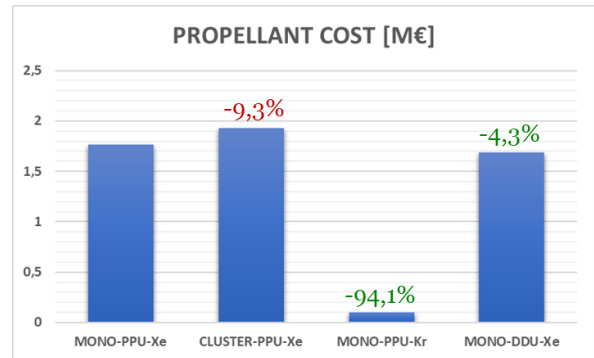


**Figure 8: Propellant cost comparison, SET-1.**

The optimal architecture is selected with respect to the score value closer to zero. The results are presented in Table 9 and demonstrate that for the operating points of SET-1 the reference architecture is the optimal one in the comparison between monolithic and cluster architecture. With the krypton vs xenon comparison, the krypton-based is selected owing due to the influence of the FoM related to the cost of the propellant. Lastly, the DDU architecture is preferable with respect to the architecture based on PPU.

**Table 9: Overall comparison results, SET-1.**

Monolithic vs Cluster		
<b>Final rank</b>	<b>-0,3025</b>	<b>-0,4317</b>
Xe vs Kr		
<b>Final rank</b>	<b>-0,5522</b>	<b>-0,4406</b>
PPU vs DDU		
<b>Final rank</b>	<b>-0,3763</b>	<b>-0,3561</b>

### 5.3. SET2 of operative points: architecture comparison results

In this section, the results obtained with the second set of operative points are presented. The comparison of the mass budgets illustrates how the advantages obtained with the higher specific impulse allowed by krypton imply a relevant reduction of the propellant mass for the case adopting this architecture (Figure 9). With respect to the reference case, the DDU architecture allows a reduction of both dry and propellant mass budgets, repeating the results obtained for the first set of operative points.

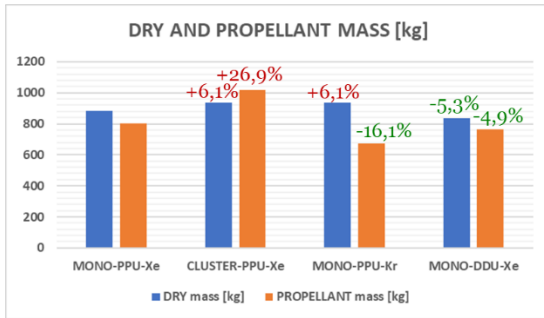


**Figure 9: Results of the Dry Mass and Propellant Mass budgets comparison, SET-2.**

For the rationale used to select the second set of operative points, the DDU case has a higher discharge power which results in an increase of the total power budget on 0,6% (see Figure 10). This increment is mainly caused by a safety margin introduced in the derivation of the power budget of the spacecraft which is proportional to the discharge power of the thruster. The selected operative point for DDU in SET-2 has a discharge power of 22,2 kW higher more than 1kW with respect to the other operative points selected for HT20k.

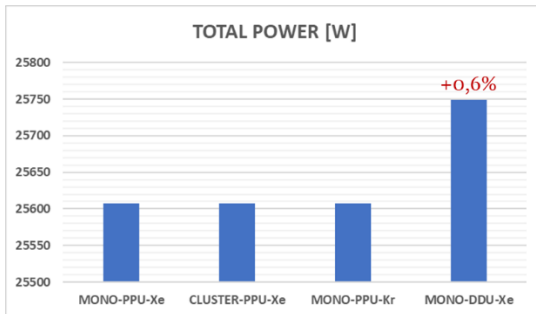


**Figure 10: Total Power Budget comparison, SET-2.**

In Figure 11, both total and outbound transfer times are shown. The cluster architecture, compared with the reference case, results in a higher transfer time, obtained due to the greater mass of the system. Despite the

propellant mass saved with the higher specific impulse with the krypton-based architecture, it results in an increase of the transfer time on about 20%, due to a lower thrust level (0.77 N with Kr vs 1 N with Xe). This caused a delay in the delivery of the satellite on its operative orbit. Moreover, the increase of the transfer time entails a corresponding increase of the time between two consecutive transfers, reducing the availability of the space tug. Nonetheless, the saving of over 94% in propellant cost results in a crucial advantage in the adoption of this architecture, as shown in Figure 12. The implementation of the cluster architecture results in the increase of the propellant cost on 25.9%.

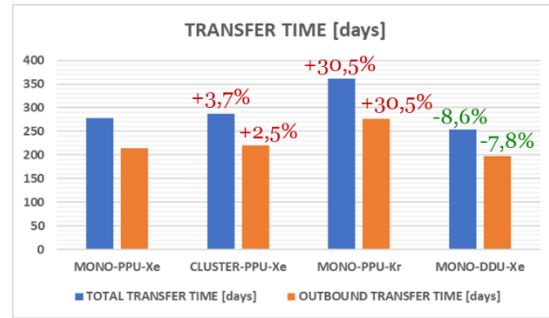


**Figure 11: Total and Outbound transfer time comparison, SET-2.**

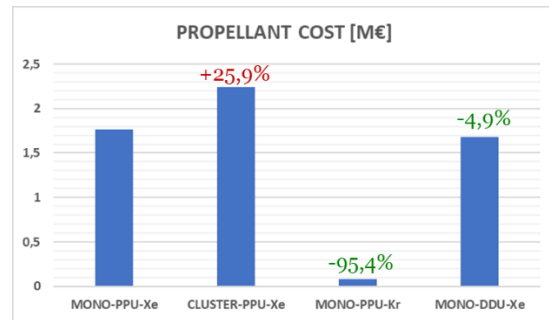


**Figure 12: Propellant cost comparison, SET-2.**

After the trade-off process was applied, the direct comparison of the architectures became possible. The results (see Table 10) demonstrate that the architecture based on the monolithic, DDU architectures with krypton propellant is the optimal solution to be adopted for this typology of mission scenario.

**Table 10: Overall comparison results, SET-2.**

	Monolithic vs Cluster	
<b>Final rank</b>	<b>-0,2359</b>	<b>-0,3697</b>
	Xe vs Kr	
<b>Final rank</b>	<b>-0,5521</b>	<b>-0,4415</b>
	PPU vs DDU	
<b>Final rank</b>	<b>-0,3794</b>	<b>-0,3553</b>

#### 5.4. Comparison among all cases

The comparison among all the analysed architecture alternatives (see Table 11), with respect to the two sets of operative points, results in the identification of the system based on krypton operation as the optimal architecture to adopt for the space tug system. In particular, the operative point at 1N, 2500s and 22.5 kW demonstrated a lower propellant mass, transfer times and propellant cost. The latter parameter plays the greater role in the selection of this case owing to a saving of over 1.6 M€ with respect to the baseline case.

**Table 11: Comparison of all the cases under analysis.**

SET	EPS arch	EPCDS arch	Prop.	SCORE	RANK
SET_1	Mono	PPU	Xe	-0,07068	5
	<b>Mono</b>	<b>PPU</b>	<b>Kr</b>	<b>-0,06532</b>	<b>1</b>
	Mono	DDU	Xe	-0,0703	3
	Cluster	PPU	Xe	-0,09218	6
SET_2	Mono	PPU	Xe	-0,07068	5
	Mono	PPU	Kr	-0,06596	2
	Mono	DDU	Xe	-0,07007	4
	Cluster	PPU	Xe	-0,09317	7

## 6. CONCLUSION

In this paper, a space tug was envisaged to provide transfer service of commercial telecommunication satellite up to the geostationary orbit (GEO). This reference scenario was selected to investigate the adoption of technologies alternative to those currently exploited. The main purpose of the research is to investigate the possibility to mitigate several criticalities of these typologies of transportation systems, mainly related to both mass and power budgets.

The analysis performed considers a trade-off between the adoption of a monolithic architecture based on a single 20 kW EPS and a cluster architecture based on multiple 5 kW EPS strings.

The propellant comparison encompasses several aspects i.e. HT performance, propellant storage conditions, tank size and volume, propellant cost and system complexity. All these factors have been evaluated comparing xenon, which is already largely used, and krypton, owing to its advantages in lower price with respect to xenon with comparable performance.

The last analyses performed at system level considers the comparison between the architecture of the EPS based on a power-processing unit (PPU) and the direct-drive (DD) approach. The latter solution allows to deliver power to the thruster directly from the solar arrays, without the need of a heavy and bulky PPU, in particular for HP-SEP. However, the implementation of a DD approach requires to develop satellite platforms with high bus voltages. In order to investigate the various system parameters and

verified the fulfilment of mission requirements and constrains, the MISS tool was updated implementing the possibility to implement DDU and alternative propellant operation. The new MAGNETO tool allows to evaluate different architecture alternatives with respect to the mission needs. The eight reference cases were chosen for the comparison of possible high-power space tug system architectures. These cases were investigated considering two different approaches for the selection of the thruster operative points. Through a trade-off analysis based on pre-determined figures of merit, the optimal solution was identified for both sets. The optimal solution was identified as the system based on a monolithic 20kW EPS string operating with a traditional PPU and krypton propellant.

Further development of this analysis will be implemented also investigating other architecture alternatives. Moreover, a greater number of the operative points will be compared, based on the experimental verification of the thruster performance maps, foreseen in SITAEL in the nearest future.

### Acknowledgments

The work described in this paper has been funded by the European Union under H2020 Programme CHEOPS-GA 730135 and by the European Space Agency under GSTP Programme, Contract 4000122232.

### References

- [1] Andreussi, T., Giannetti, V., Piragino, A., Ferrato, E., Faraji, F., Reza, Kitaeva, A., M., Andrenucci, M. "Development Status of the HT5k high-voltage model", IAC-19,C4,4,6,x53974.
- [2] Giannetti, V., Ferrato, E., Piragino, A., Reza, M., Faraji, F., Andrenucci, M. and Andreussi, T., "HT5k Thruster Unit Development History, Status and Way Forward", IEPC-2019-878.
- [3] Andreussi, T., Piragino, A., Ferrato, E., Reza, M., Faraji, F., Beccati, G., Pedrini, D., Kitaeva, A., Andrenucci, M., "HT20k Hall thruster development status", 69th International Astronautical Congress (IAC), Bremen, Germany, October 2018.
- [4] Piragino, A., Giannetti, V., Reza, M., Faraji, F., Ferrato, E., Kitaeva, A., Pedrini, D., Andreussi, T., Andrenucci, M and Paganucci, F., "Development status of SITAEL's 20kW class Hall thruster", AIAA Propulsion and Energy Forum, 2019.
- [5] Mammarella, M., Pissoni, C.A., Fusaro, R., Viola, N., Andreussi, T., Andrenucci, M., "A 20kW-class Hall Effect Thruster to Enhance Present and Future Space Missions", 69th International Astronautical Congress (IAC), Bremen Germany, October, 2018.
- [6] Pissoni, C.A., Mammarella, M., Fusaro, R., Viola, N., Andreussi, T., Rossodivita, A., Saccoccia, G., "Deep Space transportation enhanced by 20kW-class Hall Effect Thruster", 69th international



- Astronautical Congress (IAC), Bremen, Germany, October, 2018.
- [7] ISECG, “Global Exploration Roadmap”, 2018.
- [8] Rimani, J., Paussoni, C.A., Viola, N., Gonzalez del Amo, J., Saccoccia, G., “Multidisciplinary Mission and System Design Tool for a Reusable Electric Propulsion Space Tug”, 11th IAA Symposium on the Future of Space Exploration: Moon, Mars and Beyond: Becoming and Interplanetary Civilization, Turin, 2019.
- [9] Qaise, O., Moorhouse, A., Birreck, D., “Operational Concept of the First Commercial Small-Geo Based Mission,” Proceedings of SpaceOps 2012, The 12th International Conference on Space Operations, Stockholm, Sweden, 2012
- [10] Luebberstedt, H., et al. "Electra–Full Electric Propulsion Satellite Platform for GEO Missions.", 2017.
- [11] Herron, B.G., and Opjordan, “High Voltage Solar Arrays with Integral Power Conditioning,” AIAA 8th Electric Propulsion Conference, AIAA Paper 1970-1158.
- [12] Andreussi, T., Saravia, M.M., Ferrato, E. Piragino, A., Rossodivita, A., Andrenucci, M., Estublier, D. “Evaluation and Testing of Alternative Propellants for Hall Effect Thrusters”, IEPC-2017-380, 35th International Electric Propulsion, 2017.
- [13] Parissenti, G., Koch, N., Pavarin, D., Ahedo, E., Katsonis, K., Scortecci, F., Pessana, M. “Non-conventional propellants for electric propulsion applications”, Space Propulsion 2010, 1841086.
- [14] Welle R.P., “Propellant Storage Considerations for Electric Propulsion”, IEPC-91-107, 22nd International Electric Propulsion Conference, Viareggio, Italy.
- [15] Shagayda, A.A. “On Scaling of Hall Effect Thrusters”, IEPC-2013-056, 33rd International Electric Propulsion Conference, Washington DC, USA, 2013.
- [16] Wertz, J. R., Everett, D.F., Puschell, J.J., “Space mission analysis and design”, Space technology Library, 2011.
- [17] Metcalf, K.J., “Power Management and Distribution (PMAD) Model Development”, Report contract NAS2-01140
- [18] Spence, B., White, S., Wilder, N., Gregory, T., Douglas, M., Takeda, R., “Next Generation UltraFlex solar array for NASA’s New Millennium Program Space Technology 8”, IEEE Aerospace Conference Proceedings, 2005
- [19] Mercer, C. R., Kerslake, T. W., Scheidegger, R. J., Woodworth, A. A., & Lauenstein, J. M., “Solar Electric Propulsion Technology Development for Electric Propulsion”, Space Power Workshop, Huntington Beach, CA, 2015.
- [20] Zubi, G., Dufo-López, R., Carvalho, M., & Pasaoglu, G. “The lithium-ion battery: state of the art and future perspectives”, Renewable and Sustainable Energy Reviews, 89, 292-308, 2018.
- [21] SRE-PA & D-TEC, S., “Margin philosophy for science assessment studies”, 2012.
- [22] Hofer, R. R., and Randolph, T. M., “Mass and Cost Model for Selecting Thruster Size in Electric Propulsion Systems,” Journal of Propulsion and Power, vol. 29, pp. 166–176, 2013.